

Electrochemical properties of lithium/sulfur-polyacrylonitrile-carbon nanotube composite cells using ether-based electrolyte at high rate

Changhyeon Kim^a, Qing Wang^a, N. Subba Reddy^a, Huihoon Kim^a, Gyu-Bong Cho^a, Jou-Hyeon Ahn^a,
Ki-Won Kim^a, Ho-suk Ryu^b, Youngchul Kim^c, Sun-hwa Yeon^d and Hyo-Jun Ahn^{a,*}

^aDept. of Materials Engineering and Convergence Technology, Gyeongsang National University, Jinju, Korea

^bDept. of Materials & Energy Engineering, Kyungwoon University, Gumi, Korea

^cAgency for Defense Development, Yuseong, P.O. Box 35-4, Daejeon 305-600, Korea

^dKorea Institute of Energy Research, 102, Gajeong-ro, Yuseong, Daejeon 305-343, Korea

A sulfur-polyacrylonitrile-carbon nanotube (SPANC) composite is prepared by mixing and heat treatment of sulfur, polyacrylonitrile, and carbon nanotubes, with a high sulfur content of 61.94 wt%. The electrochemical properties of a Li/SPANC cell are investigated using 1,2-dimethoxyethane (ethylene glycol dimethyl ether, DME) and 1,3-dioxolane (ethylene glycol methylene ether, DOL) electrolytes. The Li/SPANC cell using the ether-based electrolytes shows high first discharge capacity of 1,037 mAh g⁻¹ at a rate of 0.1 C. And at a high rate of 1 C, it presents excellent cyclability, yielding a first discharge capacity of 500 mAh g⁻¹ and retaining 80% of this capacity at the 100th cycle.

Key words: Composites, Electrochemical properties, Energy storage.

Introduction

One of the most promising batteries for the next generation is a Li/S battery. As a cathode active material, elemental sulfur has a high theoretical specific capacity of 1,672 mAh g⁻¹. The theoretical energy density of Li/S batteries is 2,600 Wh kg⁻¹. However, Li/S batteries have the disadvantage of low utilization of the cathode active material, low rate capabilities, and low cycle life. These drawbacks are caused by the electrically insulating nature of sulfur and the loss of active material by the dissolution of lithium polysulfides [1]. To overcome these problems, sulfur-containing cathodes have been fabricated by infiltration of sulfur into mesoporous carbon [2], using hollow carbon-sulfur composites [3], and creating conducting composites of sulfur and conducting polymers [1, 4-34].

A sulfur-polyacrylonitrile (PAN) composite in particular is a good candidate for a sulfur-containing electrode material [5]. Wang *et al.* prepared a sulfur-polyacrylonitrile (S-PAN) composite by heating sulfur and PAN, exhibiting the possibilities of good electrochemical properties using carbonate-type electrolytes. [4]. Most researchers have carried out studies using carbonate-based electrolytes [1, 4-6, 8, 10, 13-17, 20, 23-25, 29-33]. Some researchers have reported the effect of different types of electrolytes on the electrochemical properties of Li/S-PAN cells

[6, 8]. Recently, ether-based electrolytes have also been studied [6, 8, 21, 22]. Zhang *et al.* [34] investigated a Li/S-PAN cell with ether-based electrolytes at a charge rate of 0.1 C, and the results showed high discharge capacity and long cycle life; however, at 1 C, initial cycling properties were not good [34]. There are few reports regarding long-term cycle performance at high rates. The inclusion of carbon nanotubes can increase the electrical conductivity of sulfur-polyacrylonitrile composites, which might improve the high rate properties of Li/S-PAN cells using ether-based electrolytes.

In this work, a sulfur-polyacrylonitrile-carbon nanotube (SPANC) composite is prepared by the mixing and heat treatment of sulfur, polyacrylonitrile, and carbon nanotubes, and the cycling properties of Li/SPANC cells using an ether-based electrolyte are investigated at high rate.

Experimental

Sulfur powder (-325 mesh, Aldrich Chem. Co.), PAN (polyacrylonitrile, $M_w = 1.5 \times 10^5$, Aldrich Chem. Co.), and MWCNT (multi-wall carbon nanotube, Hanwha Nanotech. Corp.) were used as the starting materials, with a weight ratio of 6 : 1 : 1. To prepare the SPANC composite, all the starting powders were mixed by ball milling for 5 h, and then the mixture was heated at 320 °C for 7 h in an argon atmosphere. The morphology of the SPANC composites was observed using scanning electron microscopy (SEM, Jeol, JSM-5600). The sulfur content in the composites was determined by thermo-gravimetric analysis (TGA, TA

*Corresponding author:
Tel : +82-55-772-1666
Fax: +82-55-772-2586
E-mail: ahj@gnu.ac.kr

Instruments, Q50) performed in a nitrogen atmosphere with a heating rate of $10\text{ }^{\circ}\text{C min}^{-1}$. The XRD patterns of the SPANC composite in a 2θ range from 10° to 80° were collected by X-ray diffraction (XRD, Bruker, D8 Advance).

The SPANC composite cathode was prepared by mixing 80 wt% of the SPANC composite powder, 10 wt% MWCNT, and 10 wt% β -cyclodextrin binder in distilled water. After mixing, this slurry was pasted on an aluminum foil by tape casting and dried at $60\text{ }^{\circ}\text{C}$ for 24 h. The dried slurry was used as a sulfur cathode after punching. The Li/S cell was assembled by stacking SPANC composite cathodes and Celgard 2400 microporous membranes as separators in a Swagelok-type cell. Assembly of the cell was conducted in a glove box with a high-purity argon atmosphere. The electrolyte solution was composed of 0.5 M LiTFSI (lithium bis(trifluoromethane)sulfonimide) and 0.015 M LiNO_3 salts in DME (1,2-dimethoxyethane, anhydrous, 99.5%, Aldrich)/DOL (1,3-dioxolane, anhydrous, 99.8%, Aldrich) (1 : 1, vol:vol) solvents. The electrochemical properties of the cell were evaluated using a CV (cyclic voltammogram, 0.05 mV s^{-1} , 1–3 V) and galvanostatic charge–discharge tests (1.5–2.8 V).

Results and Discussions

The SEM surface morphologies of the raw materials and the SPANC composite are shown in Fig. 1. The elemental sulfur had particle sizes below $100\text{ }\mu\text{m}$ in diameter, and the MWCNT consisted of carbon nanotubes with several tens of nanometers. PAN had secondary particles below $100\text{ }\mu\text{m}$, which were the agglomeration of sub-micron sized particles. From the surface morphology of the SPANC composite, the traces of sulfur and MWCNT could not be distinguished separately, but as lumps of the SPANC composite attached to each other. All ingredients might be integrated to form a uniform mixture where sulfur particles are regularly dispersed in the SPANC composite.

Fig. 2 shows the XRD patterns of the raw materials and the SPANC composite powder. PAN and MWCNT have broad peaks, which were related to nanocrystalline

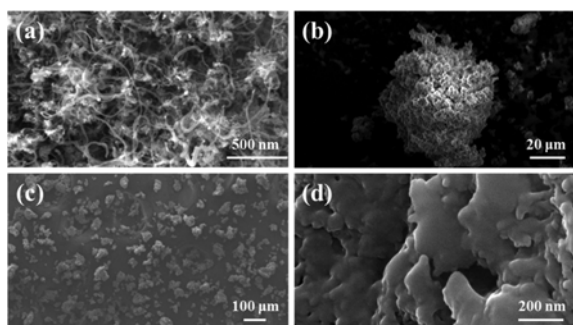


Fig. 1. SEM images of raw materials and SPANC composite; (a) MWCNT, (b) PAN, (c) elemental sulfur, and (d) SPANC composite.

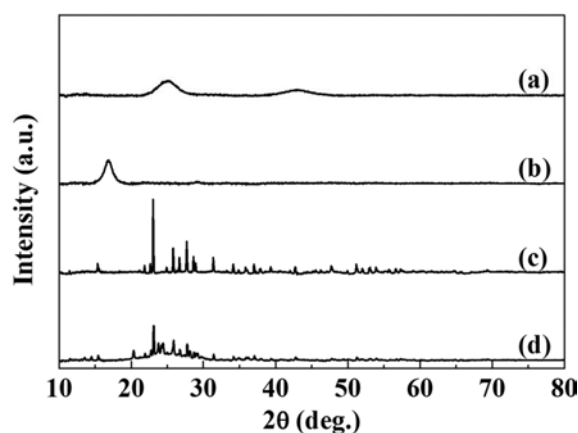


Fig. 2. XRD spectra of (a) MWCNT, (b) PAN, (c) elemental sulfur, and (d) SPANC composite.

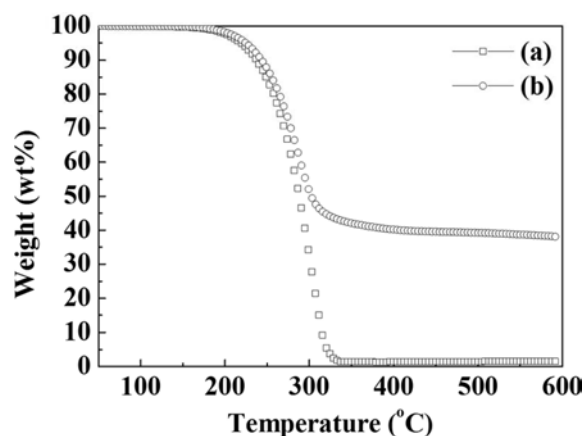


Fig. 3. TGA curves of (a) elemental sulfur and (b) SPANC composite at $10\text{ }^{\circ}\text{C min}^{-1}$.

or amorphous structures. The elemental sulfur powder has various sharp peaks of an orthorhombic structure, which was stable crystalline structure of sulfur at room temperature. The XRD patterns of the SPANC composite presents many peaks that match with those of elemental sulfur. Although some of the sulfur should evaporate after heating at $320\text{ }^{\circ}\text{C}$, the remainder exists as elemental sulfur, because of the ratio of sulfur to PAN. This result is well matched with previous reports that the elemental sulfur peaks in S-PAN composites can be detected above about 50 wt% sulfur [5, 17, 34].

Fig. 3 shows the TGA curves of elemental sulfur and the SPANC composite. The weight of sulfur decreases with heating from $200\text{ }^{\circ}\text{C}$ to $320\text{ }^{\circ}\text{C}$ and no sulfur remains above $320\text{ }^{\circ}\text{C}$ owing to evaporation. A similar trend can be observed in the SPANC composite powder. The 38.06 wt% of the original SPANC composite powder remained at $600\text{ }^{\circ}\text{C}$. From this result, the sulfur content in the SPANC composite powder was determined to be 61.94 wt%.

Cyclic voltammogram (CV) of the Li/SPANC cell was obtained, and the result is shown in Fig. 4. There are two reduction peaks at 2.34 and 2.04 V, and one oxidation peak at about 2.38 V. The CV results of the

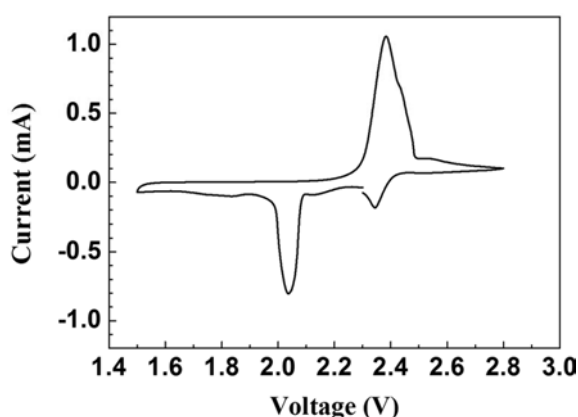


Fig. 4. Cyclic voltammogram of Li/SPANC cell at a scanning rate of 0.05 mV s^{-1} .

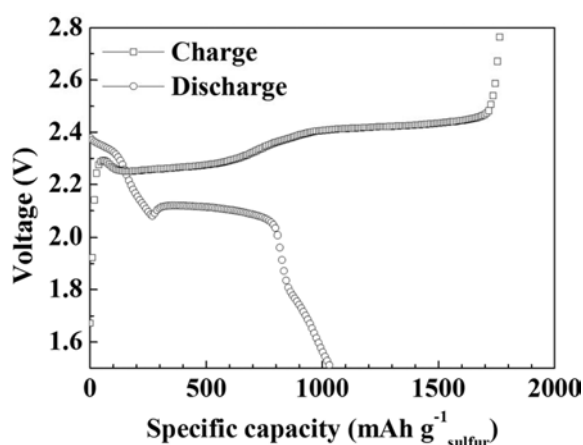


Fig. 5. Discharge and charge curves of the Li/SPANC cell at a rate of 0.1 C .

reduction reaction are similar to those of elemental sulfur electrodes using ether-based electrolytes [21, 34].

The charge-discharge curves of the SPANC composite electrode at 0.1 C are shown in Fig. 5. The discharge curve had two plateau regions at 2.3 and 2.1 V . Two plateaus at 2.25 and 2.4 V were observed during the charge process. This result coincided with the CV result in Fig. 4. However, these results were different from most previous studies [1, 4-6, 8, 10, 13-17, 19, 20, 23-25, 29-33], which showed one peak at 2.0 V during discharge. These studies used carbonate-type electrolytes, such as ethylene carbonate (EC), dimethyl carbonate (DEC), and dimethyl carbonate (DMC). Some of the studies [21, 34] showed two plateaus similar to ours with an ether-type electrolyte of DME and DOL. The upper plateau resulted from the formation of high-order lithium polysulfides such as Li_2S_n ($n > 4$), which can be dissolved into ether-type electrolytes. The electrochemical properties of the SPANC composite strongly depend on the types of electrolytes used as well as the cathode structure. The first discharge capacity is 1037 mAh g^{-1} , which is similar to a previous report [34] on Li/S-PAN cells with a similar sulfur content. This might be related to the

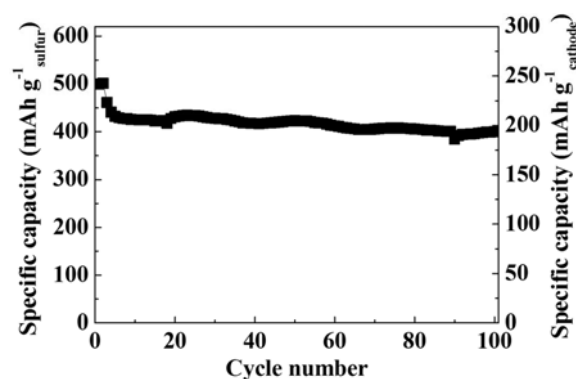


Fig. 6. Cycling performance of Li/SPANC cell at 1 C .

interaction of the sulfur cathode with MWCNT and β -cyclodextrin, which induced strong adsorption of lithium polysulfides owing to a large surface area and strong bonding nature.

Fig. 6 shows the cycling performance of the Li/SPANC cell during 100 cycles at 1 C . The first discharge capacity was 500 mAh g^{-1} and decreased to 400 mAh g^{-1} after 100 cycles, or 80% of the first discharge capacity. This Li/SPANC cell showed excellent cycle stability at high rate. This is a significant improvement compared to previous results [34].

Conclusions

A SPANC composite was prepared by the mixing and heat treatment of sulfur, polyacrylonitrile, and carbon nanotubes. From the results of XRD and TGA, it was found that elemental sulfur existed in the SPANC composite at 61.04 wt%. In CV analysis, the two reduction peaks appeared at 2.34 V and 2.04 V , owing to the use of ether-based electrolytes. The SPANC composite electrode showed a first capacity of 1037 mAh g^{-1} at 0.1 C . Moreover, at the high rate of 1 C , the first discharge capacity was 500 mAh g^{-1} , and after 100 cycles, the cell maintained 80% of its initial discharge capacity. The Li/SPANC cell with the ether-based electrolyte showed improved cycle life and rate capability because of this modification of the sulfur cathode material.

Acknowledgments

This work was supported by the three programs; 1) Next Generation Military Battery Research Center program of Defense Acquisition Program Administration & Agency for Defense Development, 2) the Global Frontier R & D Program (2013-073298) on Center for Hybrid Interface Materials (HIM) funded by the Ministry of Science, ICT & Future Planning and 3) National Research Foundation of Korea (No. 2013 R1A2A1A01015911).

References

1. X.G. Yu, J.Y. Xie, et al., *J. Electroanal. Chem.* 573 [1] (2004) 121-128.
2. X. Ji and L.F. Nazar, *J. Mater. Chem.* 20 [44] (2010) 9821-9826.
3. N. Jayaprakash, J. Shen, et al., *Angew. Chem.-Int. Edit.* 50 [26] (2011) 5904-5908.
4. J. Wang, J. Yang, et al., *Adv. Mater.* 14 [13-14] (2002) 963-965.
5. J. Wang, J. Yang, et al., *Adv. Funct. Mater.* 13 [6] (2003) 487-492.
6. J. Wang, Y. Wang, et al., *J. Power Sources* 138 [1-2] (2004) 271-273.
7. X. Yu, J. Xie, et al., *J. Power Sources* 132 [1-2] (2004) 181-186.
8. X. Yu, J. Xie, et al., *J. Power Sources* 146 [1-2] (2005) 335-339.
9. W. Pu, X. He, et al., *Ionics* 13 [4] (2007) 273-276.
10. J. Fanous, M. Wegner, et al., *Chem. Mat.* 23 [22] (2011) 5024-5028.
11. L. Wang, J. Zhao, et al., *Electrochim. Acta* 56 [14] (2011) 5252-5256.
12. W. Wei, J. Wang, et al., *Electrochem. Commun.* 13 [5] (2011) 399-402.
13. L. Yin, J. Wang, et al., *J. Mater. Chem.* 21 [19] (2011) 6807-6810.
14. T. Miyuki, T. Kojima, et al., *Sen-I Gakkaishi* 68 [7] (2012) 179-183.
15. H. Schneider, A. Garsuch, et al., *J. Power Sources* 205 (2012) 420-425.
16. J.E. Trevey, J.R. Gilsdorf, et al., *J. Electrochem. Soc.* 159 [7] (2012) A1019-A1022.
17. L. Wang, X. He, et al., *Electrochim. Acta* 72 (2012) 114-119.
18. L. Wang, X. He, et al., *J. Mater. Chem.* 22 [41] (2012) 22077-22081.
19. L. Yin, J. Wang, et al., *Energy Environ. Sci.* 5 [5] (2012) 6966-6972.
20. L. Yin, J. Wang, et al., *Chem. Commun.* 48 [63] (2012) 7868-7870.
21. T.N.L. Doan, M. Ghaznavi, et al., *J. Solid State Electrochem.* 18 [1] (2013) 69-76.
22. T.N.L. Doan, M. Ghaznavi, et al., *J. Power Sources* 241 (2013) 61-69.
23. J. Guo, Z. Yang, et al., *J. Am. Chem. Soc.* 135 [2] (2013) 763-767.
24. K. Jeddi, M. Ghaznavi, et al., *J. Mater. Chem. A* 1 [8] (2013) 2769-2772.
25. K. Jeddi, Y. Zhao, et al., *J. Electrochem. Soc.* 160 [8] (2013) A1052-A1060.
26. F. Lin, J. Wang, et al., *J. Power Sources* 223 (2013) 18-22.
27. J. Wang, Z. Yao, et al., *Adv. Funct. Mater.* 23 [9] (2013) 1194-1201.
28. L. Wang, X. He, et al., *J. Power Sources* 239 (2013) 623-627.
29. Y. Zhang, Y. Zhao, et al., *J. Electrochem. Soc.* 160 [8] (2013) A1194-A1198.
30. Y. Zhang, Y. Zhao, et al., *J. Mater. Chem. A* 1 [2] (2013) 295-301.
31. A. Konarov, D. Gosselink, et al., *J. Power Sources* 259 (2014) 183-187.
32. J. Li, K. Li, et al., *J. Power Sources* 252 (2014) 107-112.
33. J. Wang, L. Yin, et al., *ChemSusChem* 7 [2] (2014) 563-569.
34. Y.Z. Zhang, S. Liu, et al., *J. Mater. Chem. A* 2 [13] (2014) 4652-4659.